Electronic Supplementary Material (ESI) for ChemComm.

Electronic Supplementary Information

CO_2 Activation by Ligand-Free Manganese Hydrides in a Parahydrogen Matrix

Tengfei Huang,†[a] Wenjie Yu,†[a] Juanjuan Cheng, Fei Cong, Bing Xu*[a] and Xuefeng Wang*[a]

[a] *Shanghai Key Lab of Chemical Assessment and Sustainability, School of Chemical Science and Engineering, Tongji University, Shanghai 200092, China.*

E-mail: xbrare@tongji.edu.cn; xfwang@tongji.edu.cn

† Tengfei Huang and Wenjie Yu contributed equally.

Table of contents

Experimental and Computational Methods

Our experimental method for co-deposition of laser-ablated metal atoms with CO_2 diluted in solid parahydrogen matrices has been described in detail elsewhere.[S1] Briefly, a Nd:YAG laser fundamental (1064 nm, 10 Hz repetition rate with 10 ns pulse width) was focused onto a rotating metal target, which gave a bright plume reacting with CO_2/*p*-H_2 gas mixture and spreading uniformly to the 3.5 K CsI cold window cooled by a closed-cycle helium refrigerator (Sumitomo Heavy Industrious, Model RDK408D). Carbon dioxide (Shanghai Zhenxin Gas, 99.995%), isotopic $^{13}CO_2$ (Cambridge Isotopic Laboratories, 99% ^{13}C, < 1% ^{18}O), $C^{18}O_2$ (Aldrich, 97% ^{18}O) and CO_2 + $^{13}CO_2$, CO_2 + $C^{18}O_2$, CO_2 + $C^{16,18}O_2$ + $C^{18}O_2$ mixtures, together with hydrogen or deuterium (Cambridge Isotopic Laboratories, D, 99.8%) were used in various experiments. A 1:2:1 mixture of $C^{16}O_2$, $C^{16,18}O_2$, and $C^{18}O_2$ was prepared by tesla coil discharge in a 0.5 L pyrex bulb in which a full reaction was performed after 60 min from a 1:1 mixture of $C^{16}O_2$ and $C^{18}O_2$. Following deposition, MIR spectra have been recorded from 4800 to 450 cm^{-1} on a Bruker Vertex 80V spectrometer equipped with a mercury cadmium telluride (MCTB) detector at a resolution of 0.5 cm^{-1}. Afterwards, the hydrogen matrices were annealed to desired temperatures to allow further product formation. Samples were exposed to photolysis using LED light (half-wave width 5 nm, 5 W) or a mercury arc lamp (Philips, 175 W) ranging from 520 nm to 220 nm wavelength.

Complementary density functional theory (B3LYP) calculations[S2] were performed using the Gaussian 09 package.[S3] The 6-311++G(3df, 3pd) basis set[S4] were employed for all atoms. Different spin states were also explored to locate the ground-state product molecules. Harmonic vibrational frequencies were calculated analytically with zero-point energy included for the determination of reaction energies. Transition state optimizations were done using the synchronous transit-guided quasi-Newton (STQN) method and were verified through intrinsic reaction coordinate (IRC) calculations.[S5] Single-point CCSD(T)[S6]/cc-pVTZ[S7] energy calculations were performed at the B3LYP-optimized structures. Natural population analysis (NPA) was done using NBO 3.1 embedded in the Gaussian 09 package.[S8]

Table S1 Infrared absorptions (cm^{-1}) observed for products of the reactions of Mn atoms with CO_2 molecules in solid *p*-H_2

CO_2/*p*-H_2	$^{13}CO_2$/*p*-H_2	$^{12}CO_2$ + $^{13}CO_2$/*p*-H_2	$C^{18}O_2$/*p*-H_2	$C^{16}O_2$ + $C^{16,18}O_2$ + $C^{18}O_2$/*p*-H_2
		$(CO_2)MnH_2$		
1571.8	1571.8	1571.8	1571.8	1571.8
		HMnOH		
3762.6	3762.6	3762.6	3750.6	3762.6, 3750.6
1668.8	1668.8	1668.8	1668.8	1668.8
		HCO		
1864.6	1824.5	1864.6, 1824.5	1819.8	1864.6, 1819.8

Table S2 Infrared absorptions (cm^{-1}) observed for products of the reactions of Mn atoms with CO_2 molecules in solid *n*-H_2

CO_2/*n*-H_2	$^{13}CO_2$/*n*-H_2	$^{12}CO_2$ + $^{13}CO_2$/*n*-H_2	$C^{18}O_2$/*n*-H_2	$C^{16}O_2$ + $C^{18}O_2$/*n*-H_2	$C^{16}O_2$ + $C^{16,18}O_2$ + $C^{18}O_2$/*n*-H_2
			A: HMn(η^2-O_2CH)		
2947.7	2928.2	2947.7, 2928.2	2938.0	2947.7, 2938.0	2947.7, 2944.1, 2938.0
2943.7[a]	2925.1[a]	2925.1[a]	2934.3[a]		2941.3[a]
1660.5	1660.5	1660.5	1660.5	1660.5	1660.5
1542.4[a]	1503.7[a]	1542.4[a], 1503.7[a]	1520.6[a]	1542.4[a], 1520.6[a]	1542.4[a], 1532.4[a], 1520.6[a]
1538.7	1500.2	1538.7, 1500.2	1517.0	1538.7, 1517.0	1538.7, 1528.6, 1517.0
1363.1	1339.7	1363.1, 1339.7	1328.6	1363.1, 1328.6	1363.1, 1346.4, 1328.6
1307.7	1307.2	1307.7, 1307.2	1296.7	1307.7, 1296.7	1307.7, 1299.8, 1296.7
1305.3[a]	1304.4[a]		1293.4[a]	1305.3[a], 1293.4[a]	
817.6	811.3	817.6, 811.3	780.5	817.6, 780.5	817.6, 799.3, 780.5
816.0[a]	809.6[a]	816.0[a], 809.6[a]	779.0[a]	816.0[a], 779.0[a]	797.6[a]
			B: Mn(η^2-O_2CH)		
2929.4	2909.7		2919.1		
1533.5	1495.0	1533.5, 1495.0	1512.2	1533.5, 1512.2	1533.5, 1523.7, 1512.2
1361.4	1337.9	1362.7, 1361.4	1325.2	1361.4, 1325.2	1361.4, 1344.5, 1325.2
1310.4	1309.6	1310.4, 1309.6	1299.3	1310.4, 1299.3	
823.4	817.2	823.4, 817.2	785.7	823.4, 785.7	804.8

			$(CO_2)MnH_2$		
1589.2	1589.2	1589.2	1589.2	1589.2	1589.2
			HMnOH		
3761.9	3761.9	3761.9	3750.1	3761.9, 3750.1	3761.9, 3750.1
1668.4	1668.4	1668.4	1668.4	1668.4	1668.4
			HCO		
1864.4	1824.1	1864.4, 1824.1	1819.5	1864.4, 1819.5	

[a]The site absorptions for complex A.

Table S3 Infrared absorptions (cm^{-1}) observed for products of the reactions of Mn atoms with CO_2 molecules in solid matrix samples

CO_2/*p*-H_2	CO_2/*n*-H_2	CO_2/D_2	CO_2/H_2 + D_2 (1:1)		CO_2/HD	
A: HMn(η^2-O_2CH)		A: DMn(η^2-O_2CD)	A: HMn(η^2-O_2CH)	A: DMn(η^2-O_2CD)	A: DMn(η^2-O_2CH)	A: HMn(η^2-O_2CD)
2947.6	2947.7	2208.8	2949.1	2207.1	2949.0	2207.1
	2943.7[a]	2204.4[a]				
1660.7	1660.5	1195.1	1659.7	1195.2	1195.8	1660.6
1543.6[a]	1542.4[a]	1534.9[a]	1542.7[a]	1529.2[a]	1542.0[a]	1528.7[a]
1538.9	1538.7	1524.6	1539.6	1526.0	1538.4	1524.7
1363.1	1363.1	1329.7	1363.5	1329.4	1363.3	1329.5
1307.6	1307.7	975.3	1308.4	974.7	1308.5	974.6
1305.2[a]	1305.3[a]		1305.9[a]		1305.5[a]	
817.5	817.6	811.1	817.8	810.9	817.9	810.9
	816.0[a]					
B: Mn(η^2-O_2CH)		B: Mn(η^2-O_2CD)	B: Mn(η^2-O_2CH)	B: Mn(η^2-O_2CD)	B: Mn(η^2-O_2CH)	B: Mn(η^2-O_2CD)
2929.7	2929.4	2192.4	2931.0	2191.0	2931.3	2190.9
1533.6	1533.5	1520.5	1533.9	1520.6	1533.7	1519.5
1361.4	1361.4	1327.6	1361.6	1327.5	1361.5	1327.5
1310.3	1310.4	977.2	1311.5	976.1	1311.1	976.3
823.3	823.4					

$(CO_2)MnH_2$		$(CO_2)MnD_2$	$(CO_2)MnH_2$	$(CO_2)MnD_2$	$(CO_2)MnHD$	
1571.8	1589.2	1151.1	1588.1	1152.4	1610.9	
HMnOH		DMnOD	HMnOH	DMnOD	HMnOD	DMnOH
3762.6	3761.9	2764.0			2769.1	3758.0
1668.8	1668.4	1198.9	1666.4	1200.4	1667.2	1201.1

[a]The site absorptions for complex A.

Table S4 Calculated frequencies (cm^{-1}) for products of the reactions of Mn atoms with CO_2 molecules in solid hydrogen (values in parentheses are calculated intensities in km mol^{-1})

B3LYP								mode assignment
16−O	16−18		18−O	13−C	D_2	HD		
A: $HMn(\eta^2-O_2CH)$								
3053.2 (59)	3053.2 (59)		3053.2 (59)	3043.6 (55)	2259.8 (64)	2259.8 (63)	3053.2 (59)	C−H str
1707.9 (267)	1707.9 (267)		1707.9 (267)	1707.9 (267)	1218.7 (156)	1707.9 (269)	1218.7 (155)	Mn−H str
1567.2 (358)	1557.2 (343)		1545.3 (326)	1526.6 (332)	1552.9 (404)	1553.0 (408)	1567.1 (355)	O−C−O asym
1390.3 (119)	1371.7 (112)		1351.1 (115)	1366.0 (112)	1356.1 (88)	1356.0 (98)	1390.5 (107)	O−C−O sym
1328.3 (64)	1320.7 (75)		1317.0 (78)	1327.4 (72)	984.5 (12)	984.5 (12)	1328.3 (64)	C−H bend
821.4 (57)	803.1 (51)		784.2 (46)	814.5 (60)	814.0 (60)	814.0 (59)	821.4 (58)	O−C−O bend
B: $Mn(\eta^2-O_2CH)$								
3032.9 (82)	3032.9 (82)		3032.9 (82)	3023.5 (78)	2244.0 (81)	2244.0 (81)	3032.9 (82)	C−H str
1564.0 (234)	1554.1 (223)		1542.3 (211)	1523.4 (216)	1550.1 (274)	1550.1 (274)	1564.0 (234)	O−C−O asym
1389.3 (112)	1370.8 (106)		1349.8 (109)	1365.1 (107)	1355.7 (92)	1355.7 (92)	1389.3 (112)	O−C−O sym
1331.6 (55)	1323.8 (64)		1320.3 (66)	1330.7 (60)	986.4 (10)	986.4 (10)	1331.6 (55)	C−H bend
814.8 (60)	796.8 (54)		778.3 (49)	807.7 (64)	807.2 (62)	807.2 (62)	814.8 (60)	O−C−O bend
$(CO_2)MnH_2$								
2413.5 (801)	2398.4 (785)	2393.0 (793)	2376.8 (776)	2344.6 (758)	2413.4 (799)	2413.4 (796)	2413.5 (805)	O=C=O asym

1660.7 (66)	1660.7 (66)	1660.7 (66)	1660.7 (66)	1660.7 (66)	1177.2 (64)	1643.1 (356)	1608.4 (313)	H−Mn−H sym
1588.7 (649)	1588.7 (649)	1588.7 (649)	1588.7 (649)	1588.7 (649)	1141.3 (308)	1145.9 (197)	1170.7 (221)	H−Mn−H asym
671.9 (33)	666.7 (32)	666.8 (33)	661.6 (32)	652.8 (31)	671.7 (30)	671.7 (30)	671.9 (32)	O=C=O bend
664.0 (25)	658.5 (24)	659.0 (25)	653.5 (24)	645.5 (23)	663.2 (31)	663.2 (31)	664.0 (25)	O=C=O bend
				HMnOH				
3947.7 (91)	3947.7 (91)	3934.4 (86)	3934.4 (86)	3947.7 (91)	2876.9 (70)	2876.9 (70)	3947.7 (91)	O−H str
1708.8 (214)	1708.8 (214)	1708.7 (215)	1708.7 (215)	1708.8 (214)	1219.3 (123)	1708.7 (214)	1219.3 (124)	Mn−H str
675.5 (118)	675.5 (118)	648.9 (106)	648.9 (106)	675.5 (118)	656.4 (125)	657.6 (130)	674.4 (114)	Mn−OH str

Table S5 Comparison between the observed and calculated vibrational frequencies (cm^{-1}) and isotopic frequency ratios of the new molecules HMn(η^2-O_2CH) and Mn(η^2-O_2CH)

molecule	mode	obs (in solid *p*-H_2 or D_2)				calc			
		frequency	$R_{12/13}$	$R_{16/18}$	$R_{H/D}$	frequency	$R_{12/13}$	$R_{16/18}$	$R_{H/D}$
HMn(η^2-O_2CH)	C−H str	2947.6	1.0067	1.0033	1.3345	3053.2	1.0032	1.0000	1.3511
	Mn−H str	1660.7	1.0000	1.0000	1.3896	1707.9	1.0000	1.0000	1.4014
	O−C−O asym	1538.9	1.0257	1.0144	1.0094	1567.2	1.0266	1.0142	1.0092
	O−C−O sym	1363.1	1.0175	1.0260	1.0251	1390.3	1.0178	1.0290	1.0252
	C−H bend	1307.6	1.0005	1.0085	1.3407	1328.3	1.0007	1.0086	1.3492
	O−C−O bend	817.5	1.0078	1.0474	1.0079	821.4	1.0085	1.0474	1.0091
Mn(η^2-O_2CH)	C−H str	2929.7	1.0068	1.0036	1.3363	3032.9	1.0031	1.0000	1.3516
	O−C−O asym	1533.6	1.0258	1.0142	1.0086	1564.0	1.0267	1.0141	1.0090
	O−C−O sym	1361.4	1.0176	1.0272	1.0255	1389.3	1.0177	1.0293	1.0248
	C−H bend	1310.3	1.0005	1.0083	1.3409	1331.6	1.0007	1.0086	1.3500
	O−C−O bend	823.3	1.0076	1.0477		814.8	1.0088	1.0469	1.0094

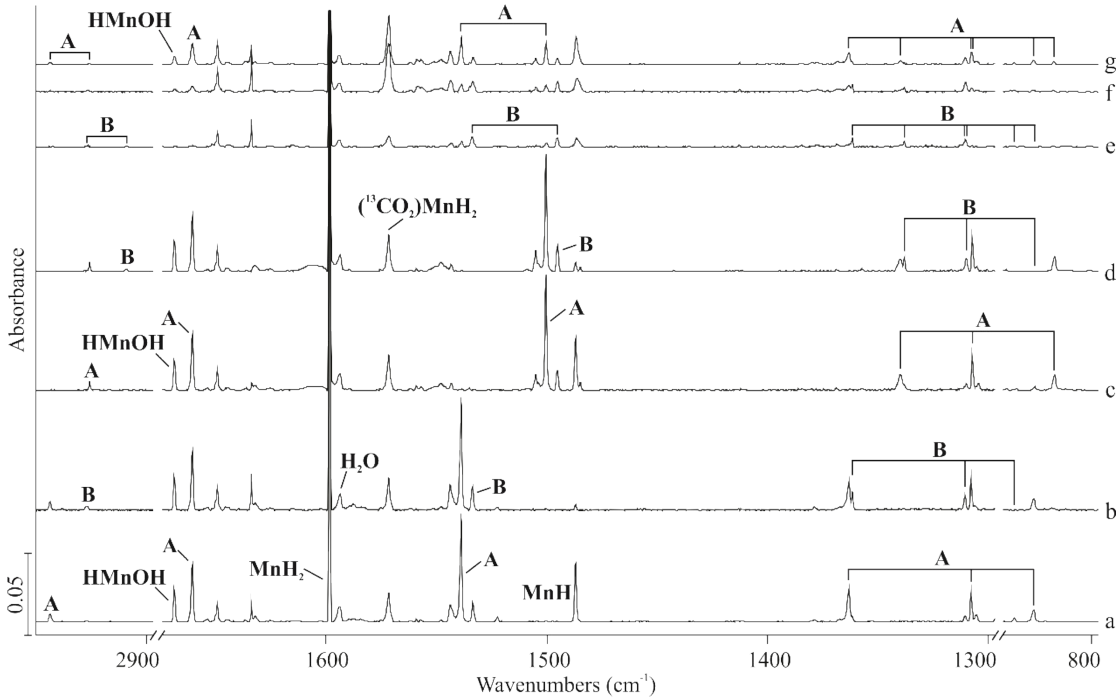

Fig. S1 Infrared spectra for the reaction products of manganese atoms and CO_2 in solid *p*-H_2 at 4 K. Mn + 0.5% $^{12}C^{16}O_2$: (a) after > 220 nm irradiation (10 min) and (b) after 450 nm irradiation (20 min). Mn + 0.5% $^{13}C^{16}O_2$: (c) after > 220 nm irradiation (10 min) and (d) after 450 nm irradiation (20 min). Mn + 0.5% $^{12}C^{16}O_2$ + 0.5% $^{13}C^{16}O_2$: (e) after 520 nm irradiation (20 min), (f) after 365 nm irradiation (5 min), and (g) after > 220 nm irradiation (5 min).

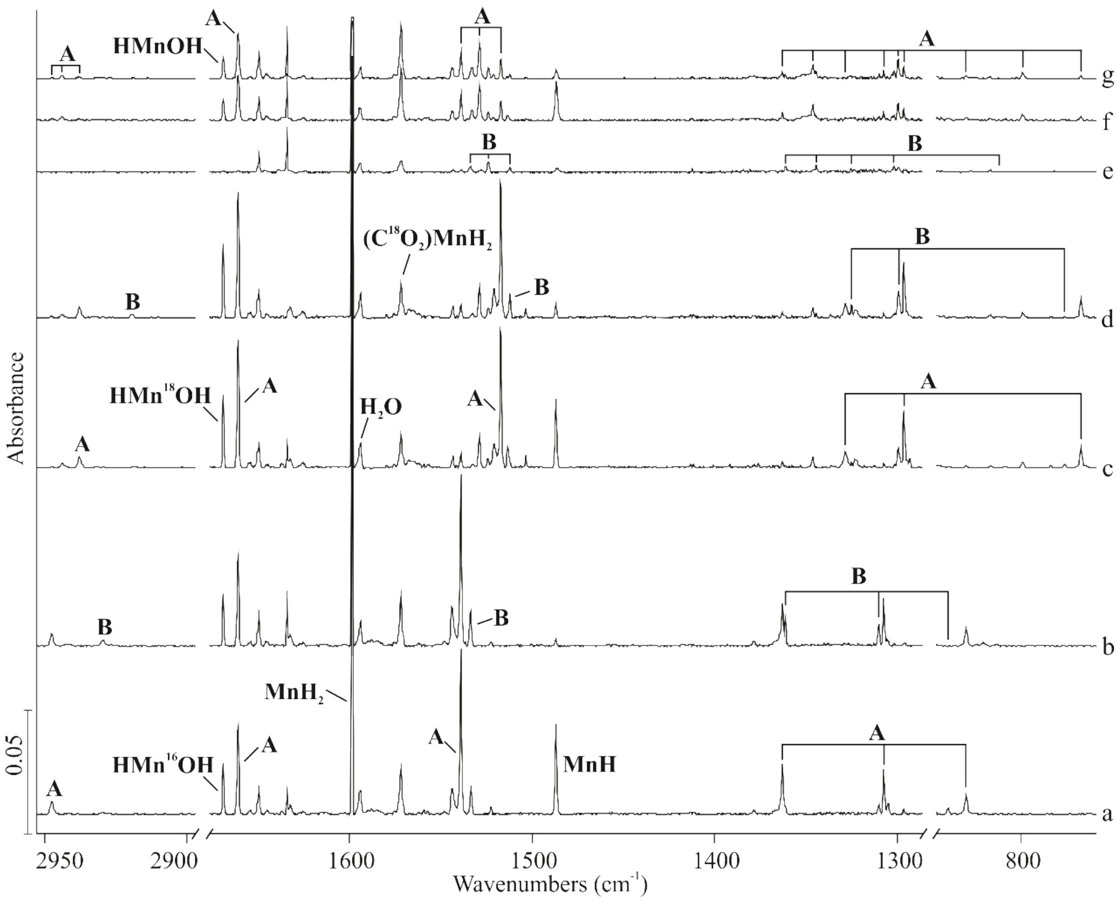

Fig. S2 Infrared spectra for the reaction products of manganese atoms and CO_2 in solid *p*-H_2 at 4 K. Mn + 0.5% $^{12}C^{16}O_2$: (a) after > 220 nm irradiation (10 min) and (b) after 450 nm irradiation (20 min). Mn + 0.5% $^{12}C^{18}O_2$: (c) after > 220 nm irradiation (10 min) and (d) after 450 nm irradiation (20 min). Mn + 1.5% ($^{12}C^{16}O_2$ + $^{12}C^{16}O^{18}O$ + $^{12}C^{18}O_2$): (e) after 520 nm irradiation (20 min), (f) after > 220 nm irradiation (10 min), and (g) after 450 nm irradiation (20 min).

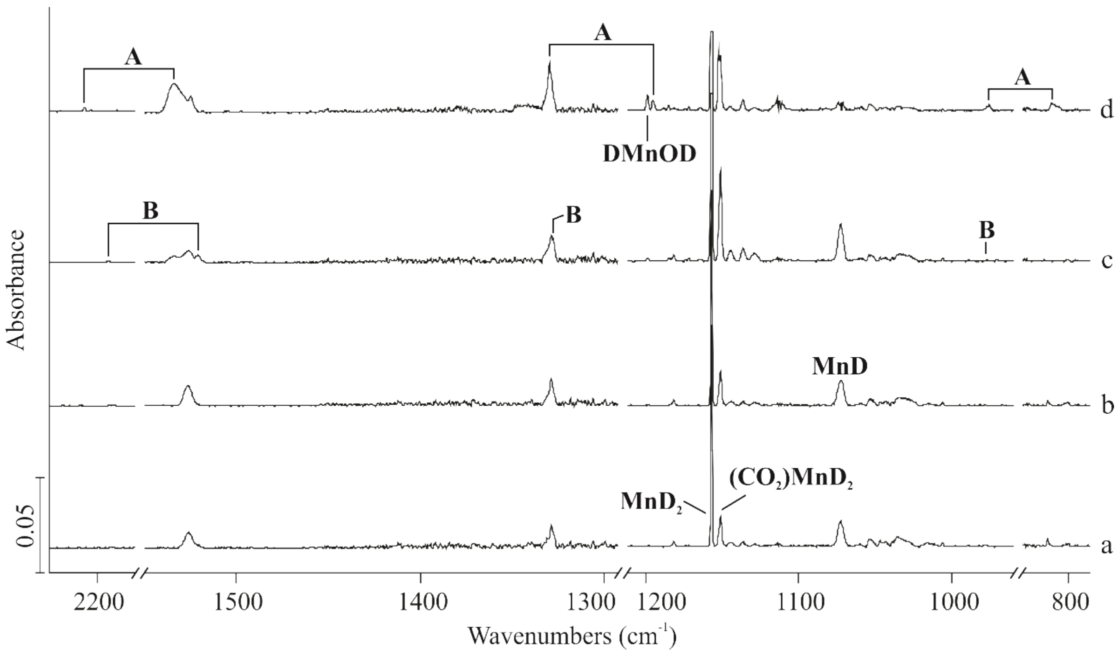

Fig. S3 Infrared spectra for the reaction products of manganese atoms and 0.5% CO_2 in solid D_2 at 4 K: (a) after deposition for 60 min, (b) after annealing to 8 K, (c) after 365 nm irradiation (5 min), and (d) after > 220 nm irradiation (10 min).

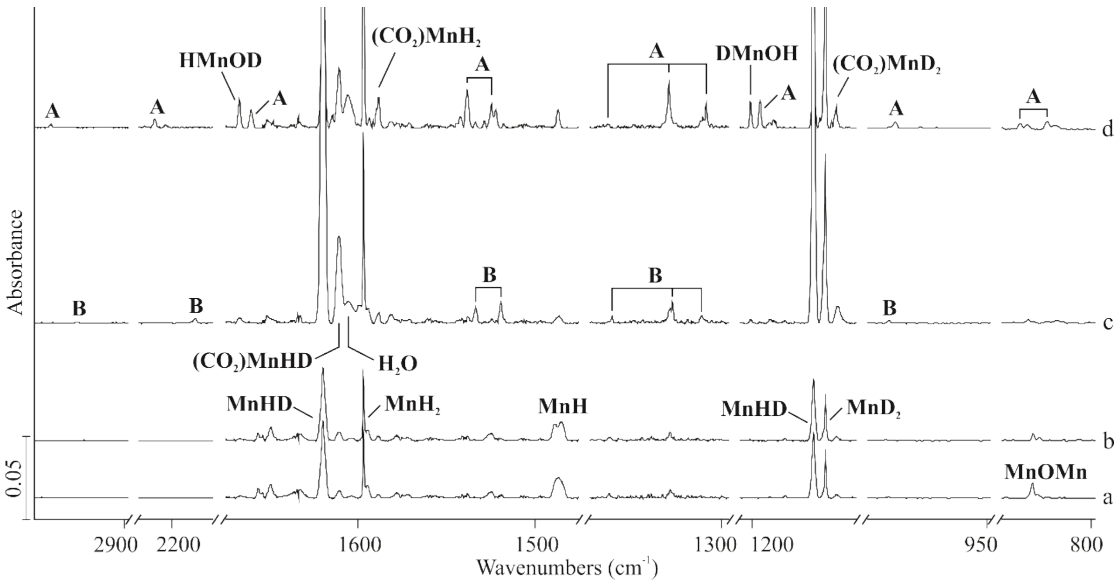

Fig. S4 Infrared spectra for the reaction products of manganese atoms and 0.4% CO_2 in solid HD at 4 K: (a) after deposition for 60 min, (b) after annealing to 6.5 K, (c) after 365 nm irradiation (5 min), and (d) after > 220 nm irradiation (10 min).

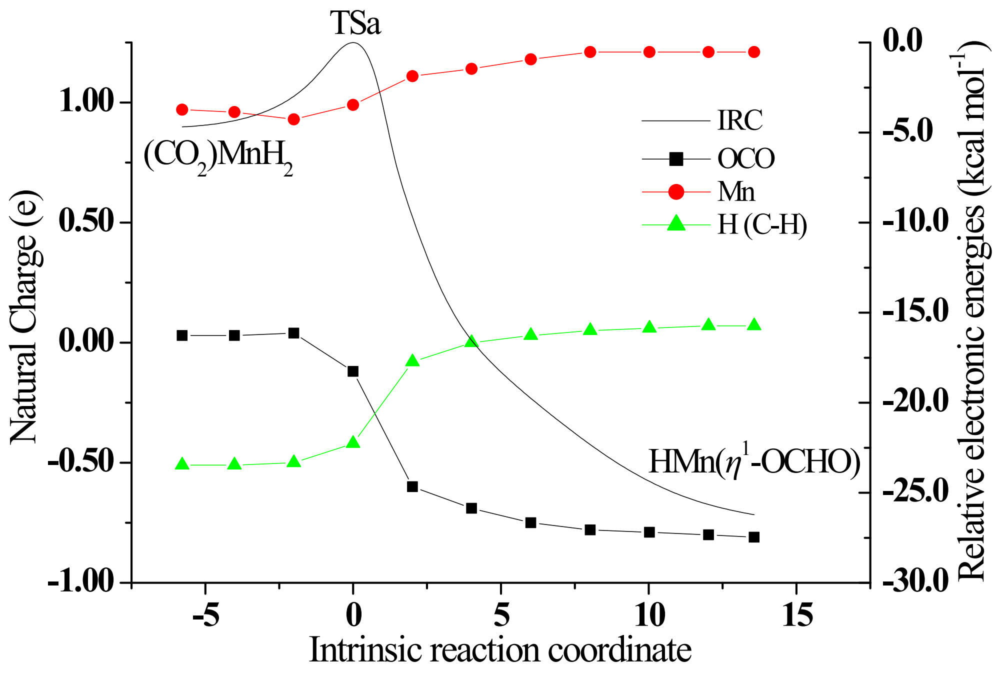

Fig. S5 IRC pathway for the transition state that connects the initial complex formed by interaction of reactants MnH_2 and CO_2 to the HMn(η^1-OCHO) minimum, and the evolution of the natural charge from natural population analysis (NPA) in hydride transfer calculated at the B3LYP/6-311++G(3df,3pd) level.

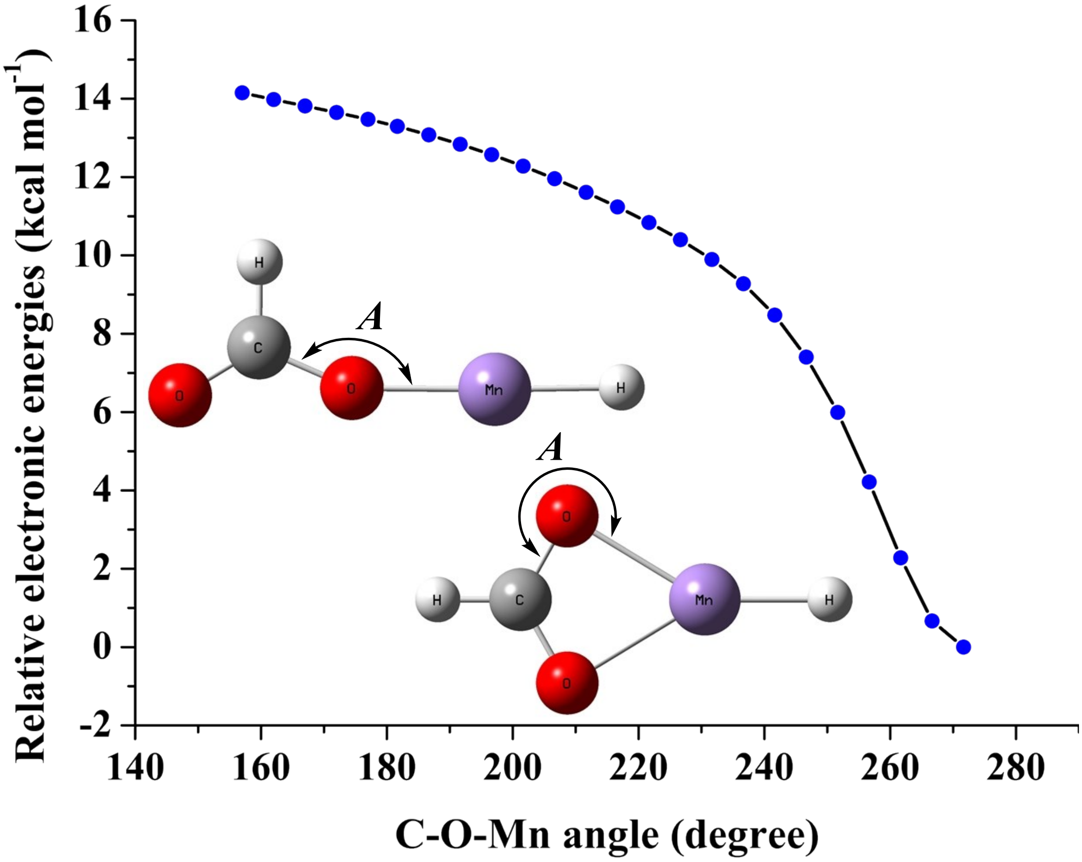

Fig. S6 Relaxed scan of the C–O–Mn angle (*A*) of the HMn(η^1-OCHO) minimum.

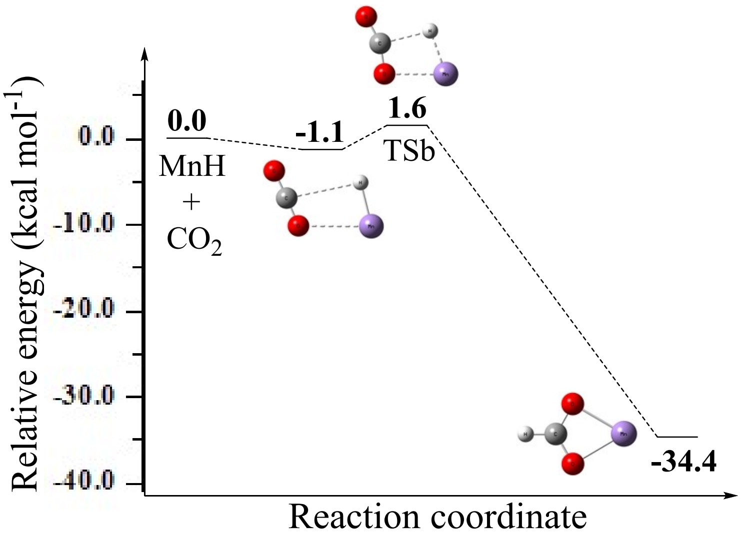

Fig. S7 Potential energy surface calculated for the reaction of MnH with CO_2.

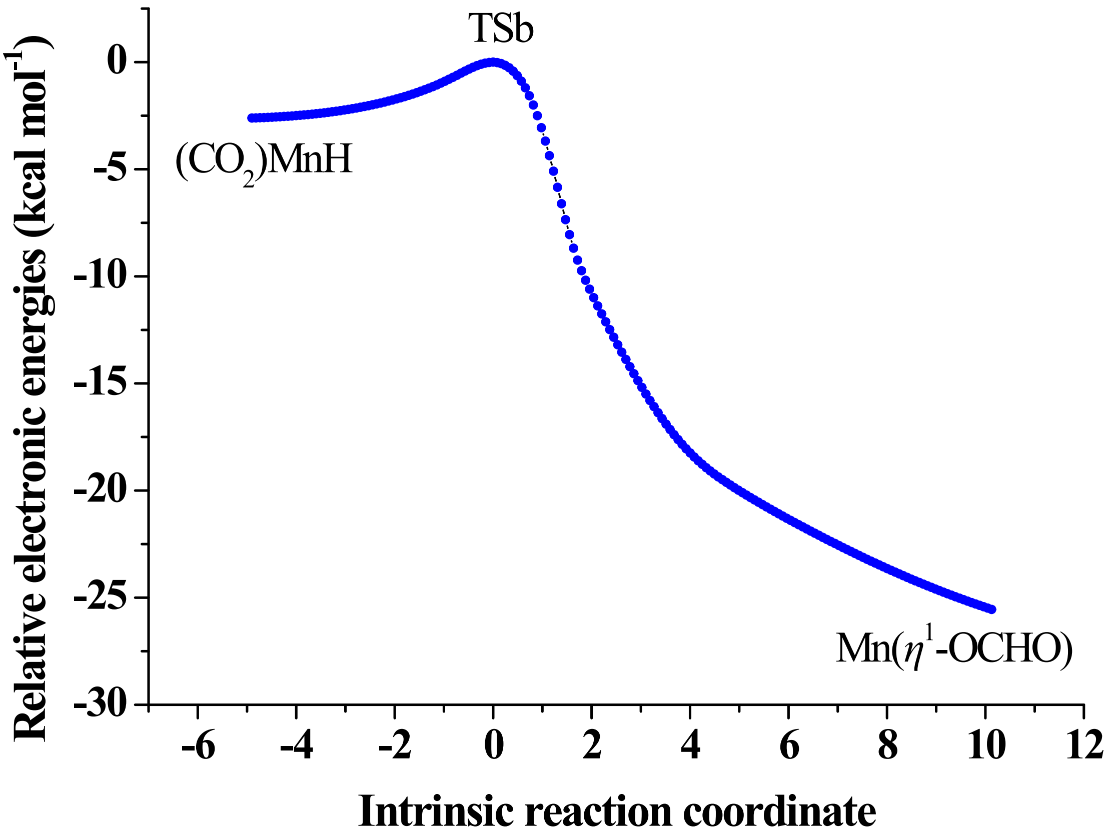

Fig. S8 IRC pathway for the transition state that connects the initial complex formed by interaction of reactants MnH and CO_2 to the Mn(η^1-OCHO) minimum.

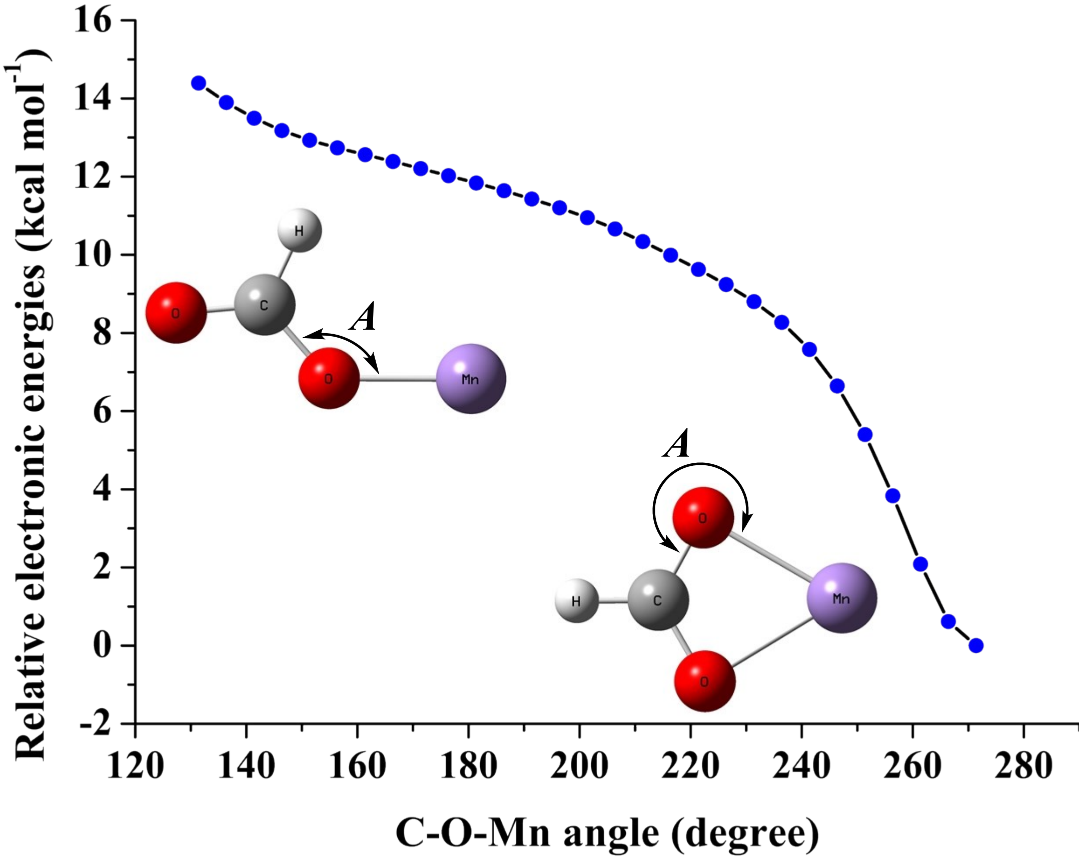

Fig. S9 Relaxed scan of the C–O–Mn angle (*A*) of the Mn(η^1-OCHO) minimum.

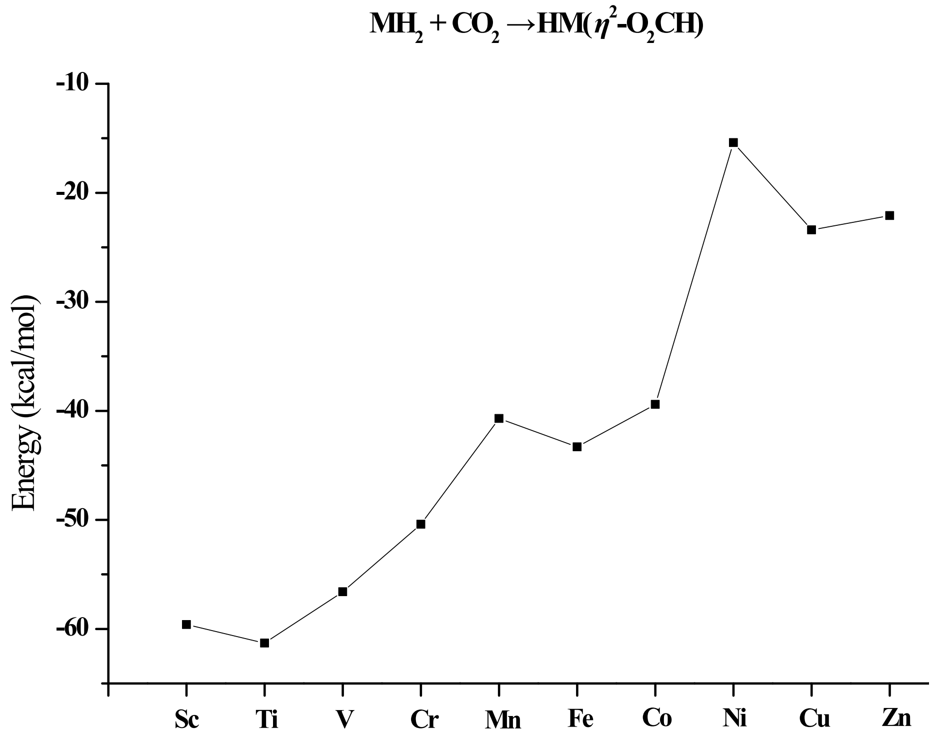

Fig. S10 The changes in energy for the reactions of MH_2 with CO_2 (M = first-row transition metal) obtained by single-point CCSD(T)/cc-pVTZ energy calculations at the B3LYP-optimized geometries.

References

S1. (a) L. Andrews, *Chem. Soc. Rev.*, 2004, **33**, 123-132; (b) W. J. Yu, X. Liu, B. Xu, X. P. Xing and X. F. Wang, *J. Phys. Chem. A*, 2016, **120**, 8590-8598.

S2. (a) C. T. Lee, W. T. Yang and R. G. Parr, *Phys. Rev. B*, 1988, **37**, 785-789; (b) A. D. Becke, *J. Chem. Phys.*, 1993, **98**, 5648-5652.

S3. M. J. Frisch, G. W. Trucks and H. B. Schlegel, GAUSSIAN 9 (Revision C.01), Gaussian Inc., Wallingford, CT, 2010.

S4. M. J. Frisch, J. A. Pople and J. S. Binkley, *J. Chem. Phys.*, 1984, **80**, 3265-3269.

S5. K. Fukui, *J. Phys. Chem.*, 1970, **74**, 4161-4163.

S6. (a) P. J. Knowles, C. Hampel and H. J. Werner, *J. Chem. Phys.*, 1993, **99**, 5219-5227; (b) M. J. O. Deegan and P. J. Knowles, *Chem. Phys. Lett.*, 1994, **227**, 321-326; (c) P. J. Knowles, C. Hampel and H. J. Werner, *J. Chem. Phys.*, 2000, **112**, 3106-3107.

S7. (a) T. H. Dunning, *J. Chem. Phys.*, 1989, **90**, 1007-1023; (b) N. B. Balabanov and K. A. Peterson, *J. Chem. Phys.*, 2005, **123**, 064107.

S8. A. E. Reed, L. A. Curtiss and F. Weinhold, *Chem. Rev.*, 1988, **88**, 899-926.